Evaluation of Retinal Nerve Fiber Layer and Ganglion Cell Layer Thickness in Alzheimer's Disease Using Spectral-Domain Optical Coherence Tomography

Ermengarda Marziani,[1] Simone Pomati,[2] Paola Ramolfo,[1] Mario Cigada,[1] Andrea Giani,[1] Claudio Mariani,[2] and Giovanni Staurenghi[1]

[1]Eye Clinic, Department of Biomedical and Clinical Sciences "Luigi Sacco," University of Milan, Milan, Italy
[2]Centre for Research and Treatment on Cognitive Dysfunctions, Neurology Clinic, Department of Clinical Science "Luigi Sacco," Luigi Sacco Hospital, University of Milan, Milan, Italy

Correspondence: Giovanni Staurenghi, Eye Clinic, Luigi Sacco Hospital, University of Milan, Via G.B. Grassi, 74-20157 Milano, Italy; giovanni.staurenghi@unimi.it.

Submitted: March 16, 2013
Accepted: July 30, 2013

Citation: Marziani E, Pomati S, Ramolfo P, et al. Evaluation of retinal nerve fiber layer and ganglion cell layer thickness in Alzheimer's disease using spectral-domain optical coherence tomography. *Invest Ophthalmol Vis Sci*. 2013;54:5953–5958. DOI:10.1167/iovs.13-12046

Purpose. To evaluate differences between the retinal nerve fiber layer (RNFL) thickness and RNFL + ganglion cell layer (GCL) thickness in patients affected by Alzheimer's disease (AD) and healthy patients using spectral-domain optical coherence tomography (SD-OCT).

Methods. This was a case-control prospective study. Twenty-one AD patients and 21 healthy subjects underwent neurological examination, clock-drawing test (CDT), Mini Mental State Examination (MMSE), and comprehensive ophthalmic evaluation with visual acuity. SD-OCT examination was performed using Spectralis and RTVue-100. An RNFL thickness map was obtained using the Spectralis volume protocol with 19 lines on the 30° field centered on the macula. On each B-scan, the outer RNFL limit was manually set. Statistical analysis was performed to assess interoperator RNFL evaluation thickness. An RNFL+GCL thickness map was obtained using the RTVue-100 MM6 protocol. Maps were divided into the nine ETDRS subfields and each map value in every area was evaluated. A single eye from each patient was randomly chosen to perform the analysis. Differences between AD and healthy subjects were assessed.

Results. The two study groups were age and sex matched. MMSE results were 19.9 ± 3.1 and 27.9 ± 1.3, respectively ($P < 0.001$). There was good agreement in the manual delimitation of the RNFL layer. There was a significant difference in the thickness of both the RNFL and the RNFL+GCL in all examined fields. For example, in the inferior internal subfield, the RNFL thickness was 28.1 ± 3.1 μm for AD patients and 32.6 ± 3.8 μm for healthy subjects ($P < 0.001$).

Conclusions. These results indicate that RNFL and RNFL+GCL thickness measurements are reduced in AD patients compared with healthy subjects. This finding may represent a useful element for the diagnosis and follow-up of this pathology.

Keywords: Alzheimer's disease, SD-OCT, RNFL, GCL

A reduction of visual acuity, color blindness, and alteration of spatial resolution has been reported in patients affected by Alzheimer's disease (AD).[1,2] Although an involvement of posterior visual pathways and primary and associative visual cortices might explain most of these symptoms,[3–12] the retina may also play a role. In fact, retinal pathology in AD was demonstrated in a postmortem series,[13,14] with ganglion cell loss in foveal and parafoveal retinas. Amyloid plaques were recently revealed in the retina of subjects who died with AD.[15] Few studies[16–25] have evaluated retinal structure and function in vivo in patients with AD, but the results so far have been controversial. One of the major sources of inconsistency in these studies lies in the variability of the techniques used, which vary from ERG[22–24,26–28] to optical coherence tomography (OCT),[17,20–25] scanning laser polarimetry (SLP),[18] and Heidelberg retinal topograph (HRT).[16] Another reason for inconsistent results might be because most research has been conducted on the peripapillar area,[20–23,25] whereas only one study has evaluated the macular region.[17] Interestingly, in histological studies, the main alterations were found in the macular area.[13,14]

In this study, we use spectral-domain OCT (SD-OCT), which is one of the latest techniques used in retinal evaluation[29–32] for studying the macular region of patients with AD. We hope to bring some light on this disputed issue and to identify a noninvasive biological marker of the disease.

Methods

Case-Control Prospective Study Subjects

Patients were included in the study if they had a diagnosis of probable AD according to the National Institute for Neurological and Communicative Disorders and Stroke–Alzheimer's Disease and Related Disorders Association (NINCDS-ADRDA) criteria,[33] with mild-to-moderate dementia (Mini-Mental State Examination[34] between 15 and 26).

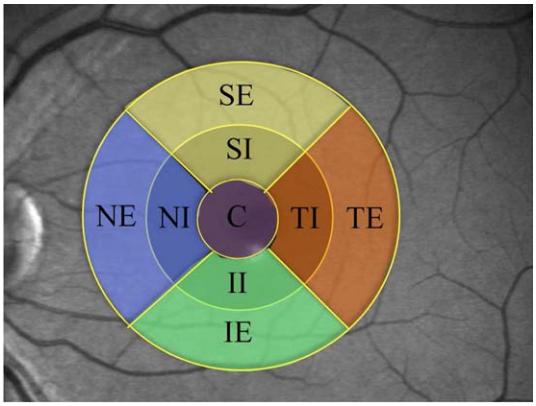

FIGURE 1. The map was divided into the nine ETDRS macular fields. C, central sector; SI, superior internal sector; TI, temporal internal sector; II, inferior internal sector; NI, nasal internal sector; SE, superior external sector; TE, temporal external sector; IE, inferior external sector; NE, nasal external sector.

Control subjects did not have a history of alcohol abuse, and were not affected by dysmetabolic diseases, psychiatric disorders, or other neurological pathologies potentially responsible for cognitive decline. All subjects underwent a complete ophthalmologic examination, including assessment of visual acuity, refraction, ocular motility, pupillary reflexes, anterior and posterior segment biomicroscopy, applanation tonometry, and dilated fundus examination. All participants had a corrected visual acuity of 20/40 or better with a refractive error between ±3 spheric diopters and IOPs less than 22 mm Hg. Eyes with ocular pathologies, such as glaucoma, propionic acidosis, choroidal neovascularization, AMD, retinal vascular diseases, vitreo-retinal diseases, macular hole, or patients with media opacification, such as cataract that prevented ocular and OCT examination were excluded.

Informed consent was obtained from all the patients or from their legal representatives when appropriate. The research followed the tenets of the Declaration of Helsinki and the protocol was approved by the "Luigi Sacco" Hospital ethics committee.

OCT

SD-OCT examination was performed after pupil dilatation with 1% tropicamide. Two instruments were used to evaluate retinal thickness: RTVue-100 (Optovue, Inc., Fremont, CA) and Spectralis HRA (Heidelberg Engineering, Heidelberg, Germany). The RTVue-100 allows for the measurement of the thickness of the inner retinal layer as a whole (retinal nerve fiber layer and ganglion cell layer combined [RNFL+GCL]), whereas Spectralis allows for the assessment the RNFL thickness alone.

FIGURE 2. SD-OCT image acquired with Spectralis. *Red lines* indicate the RNFL. The software identifies the internal retinal limit automatically. External RNFL limit is manually set (m).

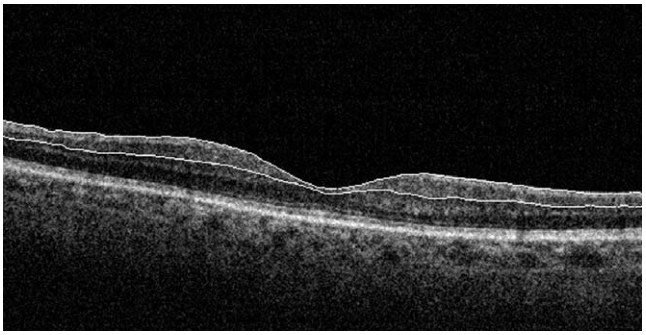

FIGURE 3. SD-OCT image acquired with Optovue RTVue-100. On each B-scan the instrument automatically sets the RNFL + GCL limits (*white lines*).

Mean thickness values of the study layer were assessed for all the subfields in the Early Treatment Diabetic Retinopathy Study (ETDRS) map for both instruments.[35] The concentric circle diameters are of 1 mL in the fovea, 3 mL in the parafoveal region, and 6 mL in the perifoveal region for both instruments (Fig. 1).

For the Spectralis, a macular thickness map was obtained using the volume protocol with 19 lines on the 30° field centered on the macula using the high-resolution modality (1476 A-scans/B-scan). The instrument was set on simultaneous infrared and SD-OCT modality. The patient was asked to fixate on a blue point in the center of the field. To assess RNFL thickness, we used the Heidelberg built-in software. Normally the software measures the retinal thickness by automatically positioning the internal limit in correspondence of the inner limiting membrane, and the external limit in correspondence of the Bruch's membrane. To measure RNFL thickness, two independent operators manually moved the external limit line in correspondence to the limit between the GCL and RNFL (Fig. 2). The external retinal thickness (from the internal limit of GCL to the external limit of Bruch's membrane) was calculated by subtracting the RNFL thickness from the entire thickness.

For the RTVue-100, the RNFL+GCL thickness map was automatically obtained using the MM6 protocol. In this acquisition modality, the instrument collects 6 B-scans centered on the macula region and elaborates these images

TABLE 1. Interoperator Agreement for RNFL Thickness Measurements using Spectralis

	r	CF	rc
C	0.97	0.99	0.97
SI	0.99	0.99	0.98
TI	0.95	0.99	0.95
II	0.93	0.99	0.93
NI	0.98	0.99	0.98
SE	0.98	0.99	0.97
TE	0.97	0.99	0.96
IE	0.96	0.99	0.96
NE	0.98	0.99	0.98

The interoperator agreement was evaluated for each sector. C, central sector; SI, superior internal sector; TI, temporal internal sector; II, inferior internal sector; NI, nasal internal sector; SE, superior external sector; TE, temporal external sector; IE, inferior external sector; NE, nasal external sector. r, precision (Pearson Correlation Coefficient); CF, accuracy; rc, concordance (Lin's Concordance Correlation Coefficient). 0 = no accordance; 1 = accordance; 2 = perfect discordance

Investigative Ophthalmology & Visual Science

Table 2. Full Retinal Thickness Maps Evaluation

	RTVue-100				Spectralis			
	Controls, μm	AD, μm	AD Effect, μm	*P* Values	Controls, μm	AD, μm	AD Effect, μm	*P* Values
C	252.3 ± 19.2	244.1 ± 17.9	−8.3	0.178	283.8 ± 27.3	277.5 ± 21.7	−6.6	0.415
SI	312.1 ± 11.0	295.2 ± 18.0	−15.5	**0.002**	338.9 ± 16.2	321.8 ± 22.3	−14.5	**0.021**
TI	305.6 ± 9.2	290.2 ± 15.5	−14.2	**0.001**	329.1 ± 13.2	316.6 ± 15.3	−10.6	**0.022**
II	311.3 ± 12.2	295.5 ± 15.8	−15.5	**0.002**	335.9 ± 16.0	322.7 ± 17.1	−11.4	**0.031**
NI	310.9 ± 11.1	295.9 ± 15.1	−13.9	**0.002**	342.1 ± 13.1	327.9 ± 20.0	−11.9	**0.025**
SE	265.7 ± 10.4	254.5 ± 15.5	−10.1	**0.021**	299.7 ± 16.3	286.8 ± 18.9	−10.9	0.059
TE	266.9 ± 9.0	253.4 ± 15.1	−13.1	**0.002**	279.8 ± 13.2	267.3 ± 14.8	−11.2	**0.017**
IE	261.2 ± 11.1	251.0 ± 15.5	−10.2	**0.024**	293.6 ± 12.5	280.7 ± 17.8	−11.8	**0.022**
NE	270.8 ± 10.4	260.9 ± 14.8	−9.1	**0.035**	305.0 ± 11.4	290.8 ± 18.8	−12.9	**0.032**

The full retinal thickness was evaluated for each sector. Controls: measurements in healthy subjects (μm); AD: measurements in AD patients (μm); AD effect: reduction in AD patients for each sector (μm); *P* values in bold are statistically significant.

to obtain a thickness map of the scanned region (Fig. 3). The thickness map provides information of the entire retinal thickness (from the inner limit of RNFL to the outer limit of the RPE), the inner retinal thickness (from the inner limit of RNFL to the outer limit of the GCL), and the outer retinal thickness (from the outer limit of GCL to the outer limit of RPE). In this study, the data from the entire retinal thickness and the inner retinal thickness were evaluated; similarly to Spectralis, the outer retinal thickness was calculated by subtracting the inner thickness from the entire thickness.

Statistical Analyses

Variables were analyzed with descriptive statistics. Continuous measures are reported as mean values (± SD), while categorical measures are reported as percentages.

ANOVA test was used to analyze the difference in thickness between AD and controls. Age- and sex-matching between the two groups was tested. These factors were also included in the ANOVA analysis as covariates.

Interrater agreement was calculated with Lin's concordance correlation coefficient (CCC).[36] An alpha error less than 0.05 was considered significant for the ANOVA test.

Results

Twenty-one patients affected by AD (age 79.3 ± 5.7 years, female-male [F/M] ratio of 17/4) and 21 healthy subjects (age 77.0 ± 4.2, F/M ratio 16/5) were included in the study. No significant difference was found between groups for age and sex. MMSE was lower in AD subjects (respectively 19.9 ± 3.1 vs. 27.9 ± 1.3; $P < 0.001$). The Lin's CCC (r) showed a good concordance between the two operators in the RNFL identification (r was found for all sectors and varied from 0.93 to 0.98) (Table 1). Both instruments showed a significant difference in full retinal thickness between patients and controls in all the sectors except in the central sector (RTVue *P* value was 0.178 and Spectralis *P* value was 0.415) and for the superior external sector (Spectralis *P* value was 0.059) (Table 2). No significant difference was found using SD-OCT Spectralis in the external layers. For example, the superior external sector was 253.9 ± 15.4 μm for controls and 249.1 ± 18.9 μm for AD patients with a *P* value = 0.666 (Table 3). A significant difference appeared between two groups for all measures of RNFL and RNFL+GCL thickness (Table 4). The results showed that inner layers of the retina appeared to be reduced in AD patients using both the instruments (Table 5).

Table 3. External Retinal Thickness Maps Evaluation: Spectralis

	Controls, μm	AD, μm	AD Effect, μm	*P* Values
C	259.8 ± 26.6	258.3 ± 21.2	−1.5	0.849
SI	305.1 ± 17.7	293.3 ± 22.8	−8.9	0.166
TI	303.6 ± 13.9	295.2 ± 16.0	−6.2	0.189
II	303.3 ± 13.7	294.6 ± 17.4	−6.5	0.183
NI	312.4 ± 13.2	301.8 ± 21.2	−7.7	0.153
SE	253.9 ± 15.4	249.1 ± 18.9	−2.3	0.666
TE	250.8 ± 13.2	244.0 ± 14.9	−5.3	0.241
IE	249.6 ± 13.6	242.4 ± 16.9	−5.5	0.261
NE	246.5 ± 12.1	239.0 ± 18.1	−5.6	0.251

The external retinal thickness (from external limit of RNFL to external limit of the retina) was evaluated for each sector. Controls: measurements in healthy subjects (μm); AD: measurements in AD patients (μm); AD effect: reduction in AD patients for each sector (μm).

Discussion

In this study, we evaluated the thickness of different retinal layers in patients affected by AD, and we compared these values with those found in healthy subjects. The results showed that the inner layers of the retina appear to be reduced in AD patients. This finding confirms previous studies[16,17,21–23,25] in which the RNFL was found to be reduced in patients with AD compared with age-matched control subjects. However, these reports did not study the macular region, where the most prominent pathological alterations

Table 4. External Retinal Thickness Maps Evaluation: RTVue-100

	Controls, μm	AD, μm	AD Effect, μm	*P* Values
C	178.4 ± 11.1	179.6 ± 11.6	1.3	0.716
SI	186.0 ± 6.9	183.3 ± 14.8	−2.3	0.531
TI	185.6 ± 6.4	185.8 ± 13.2	0.4	0.899
II	185.4 ± 7.9	185.3 ± 12.5	0.2	0.953
NI	188.0 ± 8.1	187.5 ± 11.6	−0.4	0.897
SE	167.5 ± 9.3	165.2 ± 13.2	−1.8	0.625
TE	167.1 ± 7.2	163.6 ± 11.9	−3.5	0.279
IE	162.8 ± 9.7	159.5 ± 12.1	−2.9	0.419
NE	168.9 ± 8.7	166.8 ± 9.5	−1.7	0.561

The external retinal thickness evaluation (from external limit of GCL to external limit of the retina) was evaluated for each sector. Controls: measurements in healthy subjects (μm, micronmeter); AD: measurements in AD patients (μm); AD effect: reduction in AD patients for each sector (μm).

Table 5. Internal Retinal Thickness Maps Evaluation

	RTVue-100 (RNFL+GCL)				Spectralis (RNFL)			
	Controls, μm	AD, μm	AD Effect, μm	*P* Values	Controls, μm	AD, μm	AD Effect, μm	*P* Values
C	73.9 ± 11.1	64.5 ± 9.9	−9.6	**0.008**	24.0 ± 3.7	19.2 ± 3.9	−5.1	**<0.001**
SI	126.1 ± 8.0	111.9 ± 11.2	−13.2	**<0.001**	33.9 ± 3.9	28.5 ± 5.7	−5.6	**0.001**
TI	120.0 ± 7.5	104.4 ± 12.2	−14.6	**<0.001**	25.5 ± 2.9	21.3 ± 3.0	−4.3	**<0.001**
II	125.9 ± 8.6	110.2 ± 11.2	−15.7	**<0.001**	32.6 ± 3.8	28.1 ± 3.1	−4.5	**<0.001**
NI	122.8 ± 8.3	108.4 ± 11.6	−13.5	**<0.001**	29.7 ± 3.9	26.1 ± 5.5	−4.2	**0.009**
SE	98.2 ± 6.1	89.3 ± 7.3	−8.3	**<0.001**	45.8 ± 6.0	37.7 ± 6.3	−8.5	**<0.001**
TE	99.8 ± 4.8	89.8 ± 7.3	−9.6	**<0.001**	29.0 ± 2.8	23.3 ± 2.9	−5.9	**<0.001**
IE	98.4 ± 7.3	91.5 ± 7.3	−7.3	**0.004**	44.1 ± 6.3	38.2 ± 4.5	−6.3	**<0.001**
NE	101.9 ± 5.6	94.1 ± 8.5	−7.4	**0.003**	58.5 ± 7.7	51.9 ± 9.7	−7.3	**0.014**

The internal retinal thickness was evaluated for each sector. Controls: measurements in healthy subjects (μm); AD: measurements in AD patients (μm); AD effect: reduction in AD patients for each sector (μm); *P* values in bold are statistically significant.

(neuronal loss with shrunken and vacuolated cell bodies and nuclear disintegration) were found histologically.[13,14]

The evaluation of the peripapillary region can be easily assessed by using diagnostic tools routinely used for glaucoma, namely scanning laser polarimeter (GDx; Carl Zeiss Meditec, Dublin, CA), Heidelberg retina tomographer (HRT), scanning laser ophthalmoscope (SLO). However, these instruments are not suitable for testing RNFL thickness in the macular region. Recently, Valenti[37] proposed the use of high-resolution OCT in AD patients because this instrument can reduce the time of analysis acquisition. Valenti[37] also proposed analyzing the peripapillary region. Nevertheless, OCT can be used to assess retinal layer thickness also in the macular region. RNFL reduction is not a peculiar characteristic of Alzheimer's disease and is also present in other neurological diseases (e.g., optic neuritis in multiple sclerosis) and ocular affections (e.g., glaucoma).[22] In optic neuritis, a more prominent reduction was observed in the temporal RNFL.[38,39] However, temporal RNFL is the macular subfield that presents the lowest values also in the normal retina.[40] In glaucoma, RNFL reduction is not present in all fields, but is more prominent in superior and inferior sectors.[22] This differs from what was found in AD patients, where a generalized reduction in RNFL thickness was described.[22] The reduction of RNFL thickness observed in our patients could also explain a study in which patients with AD had a more severe progression of glaucomatous optic neuropathy.[41] The same disease can be more severe for a more fragile tissue. In some cases, a more prominent reduction of RNFL was found in the temporal sectors; however, whereas in some other neurological pathologies RNFL damage does not involve the entire macular region,[40] in AD, RNFL thickness appears diffusely reduced both in our study and in previous histopathological reports.[13,14]

The only study that was conducted in the macular region was able to demonstrate a reduction in the entire retinal thickness.[17] The authors were not able to demonstrate which layer was involved because they used a time-domain OCT. The decision to use two different instruments to evaluate RNFL thickness in AD patients was derived by the distinctive, and maybe complementary, possibilities offered by both machines. Although RTVue-100 allows the mechanical measurement of RNFL+GCL as a whole layer, the Spectralis permits the quantification of the RNFL separately. In this study, only the inner layers (RNFL and RNFL+GCL combined) were reduced in AD, whereas the external layers were not affected. Using the RTVue-100, a reduction of the RNFL+GCL layer was found. However, we were not able to determine which layer between RNFL and GCL was most affected by AD. In fact, the thickness of the GCL layer could not be assessed because the reflectivity of GCL and internal plexiform layer are similar and virtually identical at the operator's eye. The boundary between the two layers is detectable only in the nearest foveal region. For this reason, RTV-100 puts the external limit of the RNFL+GCL layer at the outer limit of the external plexiform layer. On the contrary, using Spectralis we were able to specifically study only the RNFL layer. It has to be noted that a comparison between the measurements obtained with the two instruments was not feasible. Several studies have demonstrated that values acquired using different instruments are not comparable.[42] A limitation of this study is that the analysis using Spectralis was based on subjective nonautomated segmentation. However, a high interrater reliability in the measurements and a high degree of correlation between the measurements taken by both instruments were demonstrated. However, using OCT, we were not able to determine if the apoptosis signal starts from the cellular body or from the axons.

Previous histopathological data[13,14] and evidence obtained through pattern ERG analyses, with alterations in amplitude and latency,[22–24,26,28] suggest that ganglion cells are directly involved in AD. These previous findings could be explained with the presence of an immunoglobuline transmembrane receptor, RAGE (receptor for advanced glycation end products), in retinal ganglion cells and microglia.[43] RAGE is involved in AD pathogenesis and acts as a mediator of beta amyloid transport in brain microcirculation. At the same time, RAGE could be a carrier of beta amyloid from the bloodstream to the optic nerve. Binding between this upregulated receptor and beta amyloid could cause dysfunction, apoptosis, and cellular death.

In conclusion, this study confirms that RNFL thickness is reduced in AD patients. This may represent an additional tool for the diagnosis of AD, in particular considering that the measurements are objective and reproducible. However, data have to be confirmed in further studies evaluating the association with other known biomarkers of the disease. In particular, it will be important to elucidate the role of retinal measurements in the workup of AD patients and in assessing the efficacy of therapies. The study indicates that SD-OCT is a noninvasive tool that can also be used in patients affected by dementia. This is an important point for the feasibility of longitudinal studies that attempt to investigate the progression of the pathology.

Acknowledgments

The authors thank Francesca Clerici, Fausto De Ruberto, and Florangela Lopriore for providing data and patient referral.

This study was presented in part at the annual meeting of the Association for Research in Vision and Ophthalmology, Fort Lauderdale, Florida, May 2009.

Optovue provided the instruments used in this study.

Disclosure: **E. Marziani**, None; **S. Pomati**, None; **P. Ramolfo**, None; **M. Cigada**, None; **A. Giani**, None; **C. Mariani**, None; **G. Staurenghi**, Heidelberg Engineering (C)

References

1. Cogan DG. Visual disturbances with focal progressive dementing disease. *Am J Ophthalmol*. 1985;100:68–72.
2. Valenti DA. Alzheimer's disease: visual system review. *Optometry*. 2010;81:12–21.
3. Cronin-Golomb A, Corkin S, Growdon JH. Visual dysfunction predicts cognitive deficits in Alzheimer's disease. *Opt Vis Sci*. 1995;72:168–176.
4. Gilmore GC, Wenk HE, Naylor LA, Koss E. Motion perception and Alzheimer's disease. *J Gerontol*. 1994;49:P52–P57.
5. Gilmore GC, Whitehouse PJ. Contrast sensitivity in Alzheimer's disease: a 1-year longitudinal analysis. *Optom Vis Sci*. 1995;72:83–91.
6. Hinton DR, Sadun AA, Blanks JC, Miller CA. Optic-nerve degeneration in Alzheimer's disease. *N Engl J Med*. 1986;315:485–487.
7. Hof PR, Vogt BA, Bouras C, Morrison JH. Atypical form of Alzheimer's disease with prominent posterior cortical atrophy: a review of lesion distribution and circuit disconnection in cortical visual pathways. *Vision Res*. 1997;37:3609–3625.
8. Kergoat H, Kergoat MJ, Justino L, Chertkow H, Robillard A, Bergman H. Visual retinocortical function in dementia of the Alzheimer type. *Gerontology*. 2002;48:197–203.
9. Mendez MF, Cherrier MM, Meadows RS. Depth perception in Alzheimer's disease. *Percept Mot Skills*. 1996;83:987–995.
10. Morrison JH, Hof PR, Bouras C. An anatomic substrate for visual disconnection in Alzheimer's disease. *Ann N YAcad Sci*. 1991;640:36–43.
11. Rizzo JF III, Cronin-Golomb A, Growdon JH, et al. Retinocalcarine function in Alzheimer's disease. A clinical and electrophysiological study. *Arch Neurol*. 1992;49:93–101.
12. Sadun AA, Bassi CJ. Optic nerve damage in Alzheimer's disease. *Ophthalmology*. 1990;97:7–8.
13. Blanks JC, Schmidt SY, Torigoe Y, Porrello KV, Hinton DR, Blanks RH. Retinal pathology in Alzheimer's disease II. Regional neuron loss and glial changes in GCL. *Neurobiol Aging*. 1996;17:385–395.
14. Blanks JC, Torigoe Y, Hinton DR, Blanks RH. Retinal pathology in Alzheimer's disease I. Ganglion cell loss in foveal/parafoveal retina. *Neurobiol Aging*. 1996;17:377–384.
15. Koronyo-Hamaoui M, Koronyo Y, Ljubimov AV, et al. Identification of amyloid plaques in retinas from Alzheimer's patients and noninvasive in vivo optical imaging of retinal plaques in a mouse model. *Neuroimage*. 2011;54:S204–S217.
16. Danesh-Meyer HV, Birch H, Ku JY, Carroll S, Gamble G. Reduction of optic nerve fibers in patients with Alzheimer disease identified by laser imaging. *Neurology*. 2006;67:1852–1854.
17. Iseri PK, Altinas O, Tokay T, Yuksel N. Relationship between cognitive impairment and retinal morphological and visual functional abnormalities in Alzheimer disease. *J Neuroophthalmol*. 2006;26:18–24.
18. Kergoat H, Kergoat MJ, Justino L, Chertkow H, Robillard A, Bergman H. An evaluation of the retinal nerve fiber layer thickness by scanning laser polarimetry in individuals with dementia of the Alzheimer type. *Acta Ophthalmol Scand*. 2001;79:187–191.
19. Kergoat H, Kergoat MJ, Justino L, Robillard A, Bergman H, Chertkow H. Normal optic nerve head topography in the early stages of dementia of the Alzheimer type. *Dement Geriatr Cogn Disord*. 2001;12:359–363.
20. Lu Y, Li Z, Zhang X, et al. Retinal nerve fiber layer structure abnormalities in early Alzheimer's disease: evidence in optical coherence tomography. *Neurosci Lett*. 2010;480:69–72.
21. Paquet C, Boissonnot M, Roger F, Dighiero P, Gil R, Hugon J. Abnormal retinal thickness in patients with mild cognitive impairment and Alzheimer's disease. *Neurosci Lett*. 2007;420:97–99.
22. Parisi V. Correlation between morphological and functional retinal impairment in patients affected by ocular hypertension, glaucoma, demyelinating optic neuritis and Alzheimer's disease. *Semin Ophthalmol*. 2003;18:50–57.
23. Parisi V, Restuccia R, Fattapposta F, Mina C, Bucci MG, Pierelli F. Morphological and functional retinal impairment in Alzheimer's disease patients. *Clin Neurophysiol*. 2001;112:1860–1867.
24. Trick GL, Barris MC, Bickler-Bluth M. Abnormal pattern electroretinograms in patients with senile dementia of the Alzheimer type. *Ann Neurol*. 1989;26:226–231.
25. Valenti DA. Neuroimaging of retinal nerve fiber layer in AD using optical coherence tomography. *Neurology*. 2007;69:1060.
26. Justino L, Kergoat M, Bergman H, Chertkow H, Robillard A, Kergoat H. Neuroretinal function is normal in early dementia of the Alzheimer type. *Neurobiol Aging*. 2001;22:691–695.
27. Katz B, Rimmer S, Iragui V, Katzman R. Abnormal pattern electroretinogram in Alzheimer's disease: evidence for retinal ganglion cell degeneration? *Ann Neurol*. 1989;26:221–225.
28. Krasodomska K, Lubinski W, Potemkowski A, Honczarenko K. Pattern electroretinogram (PERG) and pattern visual evoked potential (PVEP) in the early stages of Alzheimer's disease. *Doc Ophthalmol*. 2010;121:111–121.
29. Alam S, Zawadzki RJ, Choi S, et al. Clinical application of rapid serial fourier-domain optical coherence tomography for macular imaging. *Ophthalmology*. 2006;113:1425–1431.
30. Drexler W, Fujimoto JG. State-of-the-art retinal optical coherence tomography. *Prog Retin Eye Res*. 2008;27:45–88.
31. Galetta KM, Calabresi PA, Frohman EM, Balcer LJ. Optical coherence tomography (OCT): imaging the visual pathway as a model for neurodegeneration. *Neurotherapeutics*. 2011;8:117–132.
32. van Velthoven ME, Faber DJ, Verbraak FD, van Leeuwen TG, de Smet MD. Recent developments in optical coherence tomography for imaging the retina. *Prog Retin Eye Res*. 2007;26:57–77.
33. McKhann G, Drachman D, Folstein M, Katzman R, Price D, Stadlan EM. Clinical diagnosis of Alzheimer's disease: report of the NINCDS-ADRDA Work Group under the auspices of Department of Health and Human Services Task Force on Alzheimer's Disease. *Neurology*. 1984;34:939–944.
34. Folstein MF, Folstein SE, McHugh PR. "Mini-mental state." A practical method for grading the cognitive state of patients for the clinician. *J Psychiatr Res*. 1975;12:189–198.
35. Kinyoun J, Barton F, Fisher M, Hubbard L, Aiello L, Ferris F III. Detection of diabetic macular edema. Ophthalmoscopy versus photography-Early Treatment Diabetic Retinopathy Study Report Number 5. The ETDRS Research Group. *Ophthalmology*. 1989;96:746–750.
36. Lin LI-K. A concordance correlation coefficient to evaluate reproducibility. *Biometrics*. 1989;45:225–268.
37. Valenti DA. Alzheimer's disease and glaucoma: imaging the biomarkers of neurodegenerative disease. *Int J Alzheimers Dis*. 2011;2010:793931.
38. Costello F, Hodge W, Pan YI, Eggenberger E, Coupland S, Kardon RH. Tracking retinal nerve fiber layer loss after optic neuritis: a prospective study using optical coherence tomography. *Mult Scler*. 2008;14:893–905.

Investigative Ophthalmology & Visual Science

39. Sepulcre J, Fernandez FJ, Salinas-Alaman A, Garcia-Layana A, Bejarano B, Villoslada P. Diagnostic accuracy of retinal abnormalities in predicting disease acivity in MS. *Neurology*. 2007;68:1488–1494.
40. Takamoto T, Schwartz B. Differences by quadrant of retinal nerve fiber layer thickness in healthy eyes. *J Glaucoma*. 2002; 11:359–364.
41. Bayer AU, Ferrari F. Severe progression of glaucomatous optic neuropathy in patients with Alzheimer's disease. *Eye*. 2002;16: 209–212.
42. Giani A, Cigada M, Choudhry N, et al. Reproducibility of retinal thickness measurements on normal and pathologic eyes by different optical coherence tomography instruments. *Am J Ophthalmol*. 2010;150:815–824. Erratum in Am J Ophthalmol. 2011;151:737.
43. Wang MY, Ross-Cisneros FN, Aggarwal D, Liang CY, Sadun AA. Receptor for advanced glycation end products is upregulated in optic neuropathy of Alzheimer's disease. *Acta Neuropathol*. 2009;118:381–389.